Channel Feasibility for Outdoor Non-Line-of-Sight mmWave Mobile Communication

Sridhar Rajagopal and Shadi Abu-Surra
Dallas Technology Lab
Samsung Telecommunications America
Richardson, TX 75082 USA
{*srajagop, sasurra*}*@sta.samsung.com*

Mehrzad Malmirchegini
ECE Department
University of New Mexico
Albuquerque, NM 87131 USA
mehrzad@ece.unm.edu

***Abstract*—Due to the scarcity of spectrum below 3 GHz for wireless communications, there have been proposals to explore millimeter wave (mmWave) spectrum (3-300GHz) for commercial mobile applications. MmWave spectrum provides unique advantages such as availability of GHz bandwidth and use of antenna arrays with beamforming to compensate for path loss. While there exist well-established models for mmWave indoor non-line-of-sight (60 GHz) and mmWave outdoor line-of-sight (backhaul) communication, mmWave channels for outdoor, non-line-of-sight, mobile communication have not been explored sufficiently. We present penetration and reflection measurements for different materials and line-of-sight and non-line-of-sight measurements for outdoor mmWave mobile communication. We find that while well-known lossy objects such as human body and concrete can have poor penetration, they are good reflectors at these frequencies, enabling the receiver to capture secondary reflections for non-line-of-sight communication. We also show that a wide beam width, low gain antenna at the mobile receiver can capture more energy in scattered non-line-of-sight environments and thus, can provide more gain than a narrow beam, high gain antenna for mobile communication. Our initial measurements motivate utilizing mmWave frequencies for outdoor non-line-of-sight mobile communication.**

I. Introduction

There has been a recent interest in exploring mmWave frequencies for outdoor, mobile broadband communication for multi-Gb/s communication over several hundreds of meters [1]. The current close-to-capacity system designs in current 3G/4G cellular standards, such as LTE-A [2], make it extremely difficult to meet the ever increasing demands of higher data rate communication with limited spectrum below 3 GHz. However, cellular mobile communication in higher frequencies of mmWave spectrum can potentially provide GHz of bandwidth, enabling multi-Gb/s communication.

Moving to higher millimeter wave (mmWave) frequencies for traditional outdoor mobile communication systems have been associated with challenges such as line-of-sight (LOS) directional communication, poor RF efficiency and higher penetration loss [3]. Hence, these frequencies have been typically deployed for fixed wireless backhaul with LOS communication. However, recently, there has been an increasing interest in using mmWave frequencies for short range non-line-of-sight (NLOS) communication with multi-Gb/s data rates, especially at 60 GHz [4]. These systems have been equipped with antenna arrays to support beamforming, which compensate for the path loss and enable NLOS communication for stationary users over short distances. Channel models for mmWave communication have been well-established for outdoor fixed LOS environments such as Local Multipoint Distribution Service (LMDS) [5-7] applications and for indoor mobile environments such as 60 GHz applications [8][9]. However, deeper understanding of the mmWave channel is needed for outdoor mobile environments to understand impact of path loss, angular spread, delay spread, NLOS, beamforming and blocking issues. This is a focus of our on-going research and is discussed in this paper.

Samsung Telecommunications America was granted a 6-month experimental license from FCC at 28 GHz for measurements up to 500 m. [Call sign: WE9XVG, File number: 0203-EX-ST-2011]. We were able to operate at > 100 m distances and were able to perform path loss and angle-of-arrival (AoA) experiments. The results showed that we could capture NLOS paths and reflections via objects such as concrete and the ground, which is highly encouraging for supporting mobile communication. An important consideration for mobile communication at mmWave frequencies is the interaction of the mobile device with the human body. We found that while penetration through the human body is very poor, the hand is extremely reflective (almost as much as metal). Also, objects such as concrete, while having significant penetration loss, also provide significant reflections. In fact at these frequencies, objects look more diffused (rough), which increases the possibility of catching secondary reflections at the mobile receiver.

II. Penetration Loss Testing

Our first experiment focused on understanding the penetration loss of mmWave through common objects that are assumed to have poor penetration properties at mmWave frequencies such as wood, leaves, metal and water. We also selected two different frequencies for our testing (28 GHz and 40 GHz). The 40 GHz was selected as the upper bound of our RF signal generator. Figure 1 shows the setup for our penetration loss experiments. A 15 dBi horn antenna with 30° half-power beam width (HPBW) has been used in this setup. In order to get a good signal strength at the receiver, the measurements were done at a distance of 30 cm between the TX and RX. Since the far field effects happen at shorter distances at higher frequencies (10 λ = 10 cm @ 28 GHz), the measurements for penetration loss are reasonably accurate at 30 cm. The distance of the object to the receiver was made variable to see the impact of the proximity to the receiver for penetration loss. The RF signal generator provided a maximum output power of 10 dBm and the resulting receive power was captured by a spectrum analyzer and correlated with a power meter as well. Figure 2 shows the relative penetration loss of typical objects at 28 GHz and 40 GHz compared to free space propagation. In

978-1-4673-1881-5/12/$31.00 ©2012 IEEE

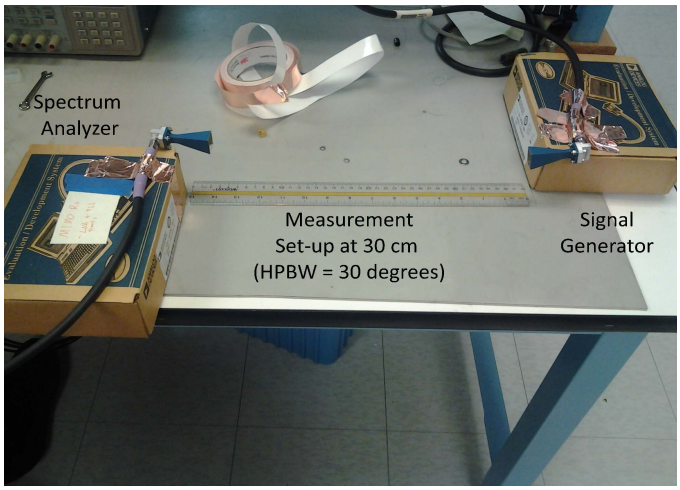

Figure 1 Setup for penetration loss measurements

order to investigate the impact of the secondary reflections on the received signal strength, the blocking objects were placed at distance 1, 2, 5 and 10 cm from the receiver. The first observation made from Figure 2 is that in general 40 GHz suffers higher penetration loss than 28 GHz. Secondly, both metal and water seem to significantly impact the penetration and can result in a 30 to 40 dB loss, if the object is very close to the receiver. As the object is moved further away, there is a higher probability that the reflected energy from other directions reach the receiver due to the reasonably wide (30° HPBW) antennas, thereby reducing the attenuation. This finding is important for the design of mobile phones since we expect the phone (which has metal) to be in close contact with the body/hand and hence, 30-40 dB loss through penetration may be difficult to accept in a system design.

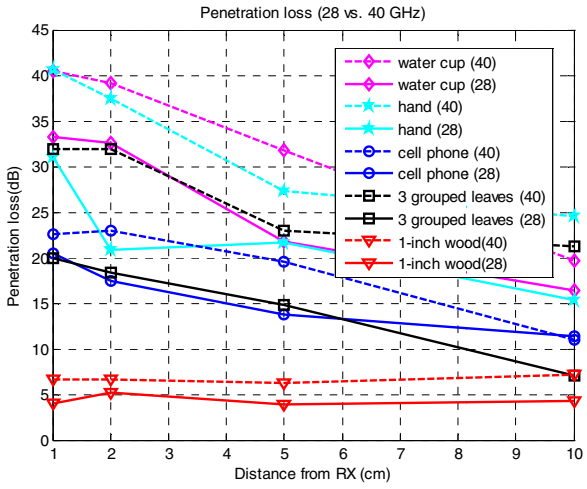

Figure 2 Penetration loss for different objects (28 vs. 40 GHz)

Given the importance of the interaction of the mobile device with the human body, we did some further analysis to understand the impact of water on the penetration loss. Figure 3 shows the impact of water and its depth on penetration loss. For this test, we also used a 60 GHz test kit from SiBeam [10] in order to compare 28, 40, and 60 GHz for penetration loss through water. Both TX and RX beams from the adaptive antenna arrays in the SiBeam kit were locked to ensure that there is no beam adaptation in the penetration measurements and the signal travels through the water before getting captured by the RX. We were able to see a 5-10 dB penetration loss per cm which was worse at higher frequencies. We also noticed a sensitivity to the shape of the object holding the water. For instance, square objects which had more uniform depth, showed greater loss than round objects, whose depth were not uniform and the maximum depth was recorded in those cases.

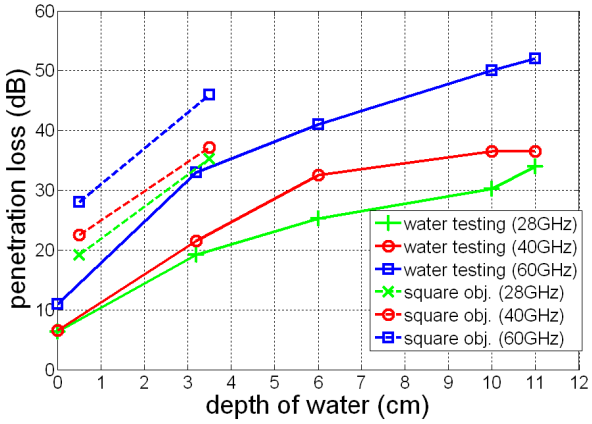

Figure 3 Water penetration loss (28 vs. 40 vs. 60 GHz)

III. Reflectivity Testing

While it became clear from the penetration tests that water and metal objects were not easy to penetrate at mmWave frequencies, there is still no explanation of the missing energy and whether it was absorbed inside the object or reflected from the object. In order to understand this further, a series of reflection tests was performed to test the reflectivity of metal and water objects. The measurement setup for reflectivity testing is as shown in Figure 4. The object was placed at a distance of 10 cm from the transmitter at boresight (0°) and the receiver was rotated at 20 cm around the object in 15° steps to capture the received power after reflection (-90° to 90°) or penetration (90° to 270°) in various directions. Both the TX and RX are pointed towards the object placed at the center at all times.

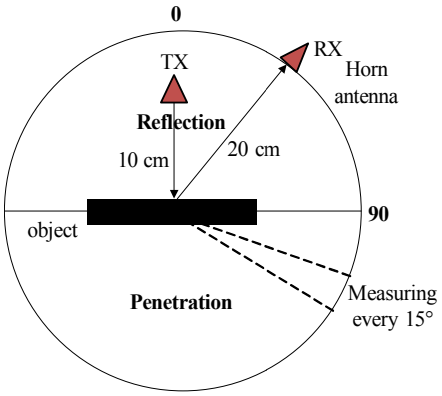

Figure 4 Measurement setup for reflectivity testing

Figure 5 and Figure 6 show the reflectivity of different materials at 28 GHz and 40 GHz respectively. The radius shows the received power in dBm with +10 dBm TX power.

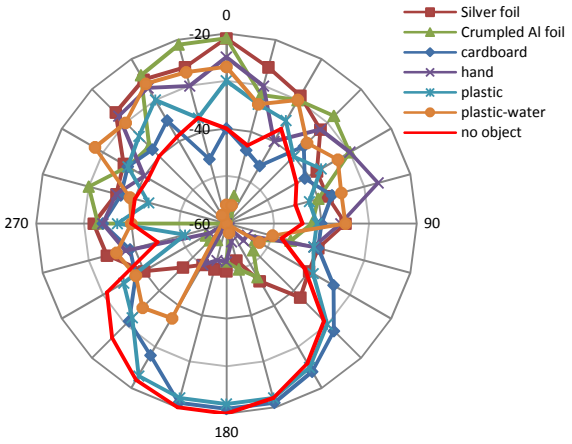

Figure 5 Reflectivity of different materials at 28 GHz

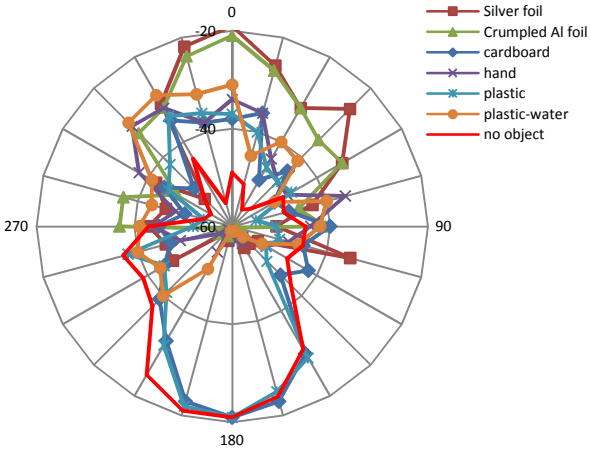

Figure 6 Reflectivity of different materials at 40 GHz

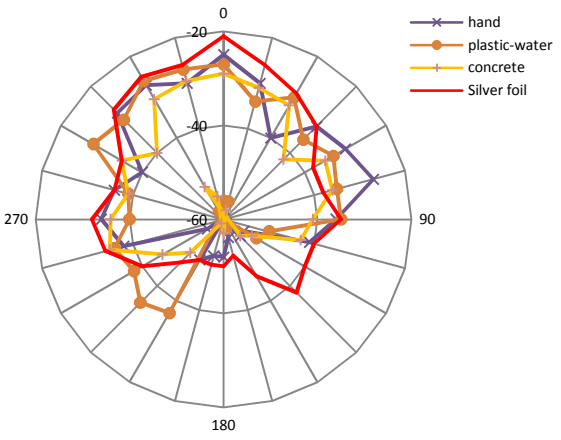

Figure 7 Reflectivity of hand, water, concrete vs. a silver foil at 28 GHz

The plastic and cardboard materials show almost no attenuation compared to free space and hence, there is little reflectivity. In contrast, hand, water, and silver foil show substantial reflections. The results were very encouraging that the hand/water objects were reflecting as much as metal objects, showing that the energy is not entirely absorbed in the object but is dispersed in the environment. Also, note that the smooth silver foil has almost as wide scattering as the crumpled silver foil showing that the reflections are highly diffused at these mmWave frequencies. Finally, the reflections are narrower at 40 GHz than at 28 GHz. This is due to the fact that a fixed horn antenna's beam width is directly proportional to wavelength. Hence, the horn has a 30% smaller beam width at 40 GHz than at 28 GHz. This may make the reflections and penetration more directional at 40 GHz.

Figure 7 shows the comparisons of reflection patterns from a silver foil, hand, water and concrete at 28 GHz in order to understand the importance of reflectivity in mobile NLOS outdoor environments. The reflectivity of hand, water and concrete are similar to that of a silver foil, which is very encouraging for the feasibility of capturing the secondary NLOS reflections at the mobile receiver for mmWave outdoor mobile communication.

IV. Outdoor Measurements

We then focused on outdoor LOS and NLOS AoA measurements to see the impact of horn antenna HPBW and elevation and azimuth angles on the received power. The antennas used for narrow and wide beam measurements are as shown in Table 1. An experimental test system was built at 28 GHz for long range outdoor measurements with a TX power output up to +30 dBm and a LNA receive gain of 22 dB. We ensured that the power amplifier (PA) and the low noise amplifier (LNA) worked in the linear region for the measurements. The output of the LNA was captured with a spectrum analyzer to measure received power. In order to characterize the behavior of mmWave for outdoor environments, we perform path loss and AoA experiments. In the subsequent parts, we present our outdoor results.

A. Path loss exponent

Figure 8 shows the received signal power (dBm) for LOS measurements up to 100m. This experiment was performed on the roof with 6° HPBW horn antennas where there were no significant reflectors apart from the ground. The path loss exponent was computed to be 1.89 which was slightly better than free space, possibly due to additional power gain from ground reflections.

Table 1 Antennas used for outdoor measurements @ 28 GHz

Antenna Gain (dBi)	Antenna HPBW	Polarization
22	6°	Linear (V)
10	55°	Linear (V)

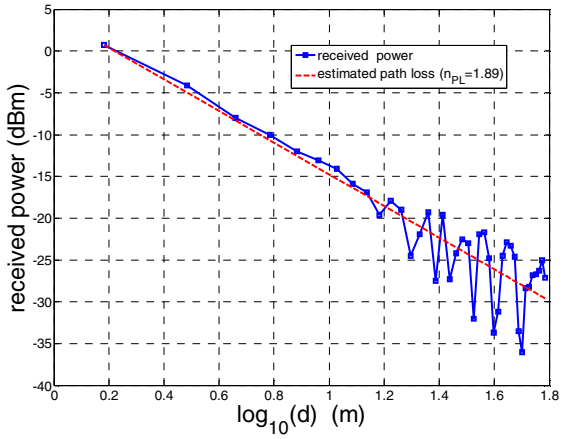

Figure 8 Path loss exponent for outdoor testing at 28 GHz.

B. *Outdoor LOS measurements*

Figure 9 shows the measurement setup for outdoor LOS measurements. The transmitter is fixed in direction, pointing at Φ_t = 0° (which is directed towards the receiver) in the azimuthal plane with a downtilt of Θ_t = -15° in elevation. Due to time and effort constraints, TX beamforming was not considered in this setup. The receiver was however, moved over the entire azimuth plane in 10° steps and both uptilting and downtilting Θ_r = -15, 0, 15° were considered in elevation. The transmit power was fixed at 29 dBm and the distance between the TX and RX was fixed at 50m. The measurements were done at both empty (LOS1) and full (LOS2) parking lots, in order to understand the impact of reflections from cars on the received signal power.

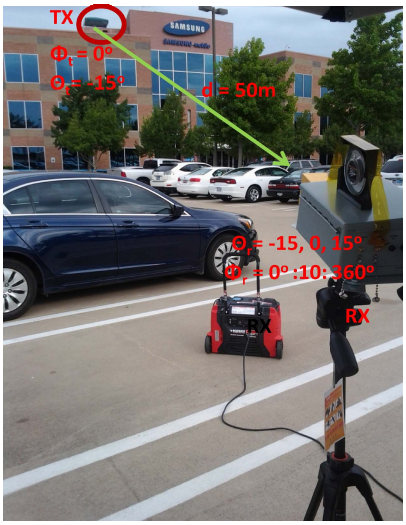

Figure 9 Measurement setup for outdoor LOS measurements

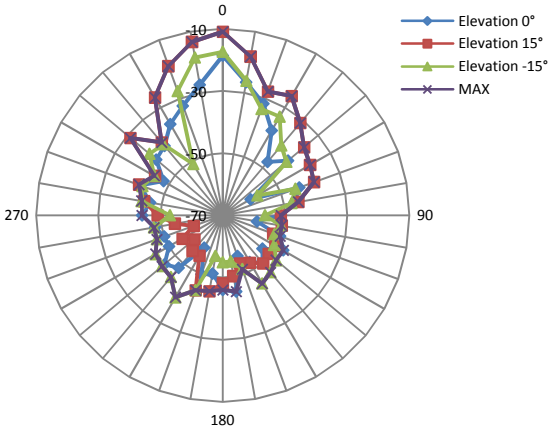

Figure 10 Antenna configuration: TX6-RX6-LOS1

Figure 10 shows the AoA measurements for 6° HPBW antenna at both TX and RX (TX6-RX6) for LOS1 and Θ_r = -15°, 0°, 15°. The MAX curve shows the maximum of all the three AoA plots, which is the gain that can be expected from an ideal RX beamformer. It can be seen that the best performance was obtained at Θ_r = 15° when Φ_r = 0° and Θ_r = -15° when Φ_r = 180°. This implies good signal strengths were received when the receiver was uptilted for LOS or the receiver was downtilted to catch the reflections from the ground in the opposite direction.

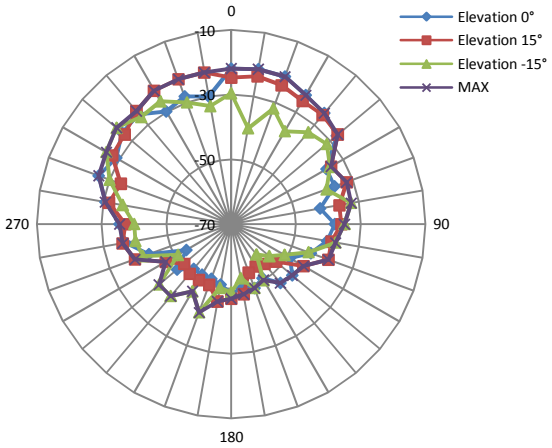

Figure 11 Antenna configuration: TX6-RX55-LOS1

Figure 11 shows the AoA measurements for 6° HPBW antenna at TX and 55° RX (TX6-RX55) for LOS1. It can be seen that the coverage is now more uniform with a wider receive antenna. This implies that there is sufficient scattering in the environment even in an empty parking lot that can be captured with a wide HPBW receive antenna. This information can be very useful in the system design for the mobile receiver to capture NLOS energy using a wide beam receive antenna.

Figure 12 compares the wide and narrow RX antennas for the empty parking lot (LOS1). Both of the measurements were done at the same location and the same transmit power and the only difference is the antenna gain and beam width. While at LOS, the narrow (6° HPBW) RX antenna provides best performance, it can be seen that the wide (55° HPBW) , low gain RX antenna provides equal or better signal power at the receiver for around 300° away from LOS even with 12 dB lower antenna gain.

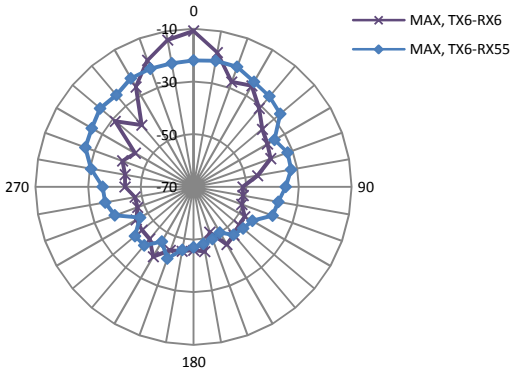

Figure 12 Comparing TX6-RX55-LOS1 and TX6-RX6-LOS1

We repeated the same set of experiments for a full parking lot (LOS2) to understand the impact of cars on the measurement results. Similar results were obtained for the full parking lot case as well. Figure 13 and 14 shows the corresponding results for narrow and wide HPBW RX antennas and the comparisons for a full parking lot. It can be seen that the full parking lot provides better coverage than empty parking lots. The reflections provide up to 15 dB more gain in certain directions, thereby helping the TX signal reach the receiver.

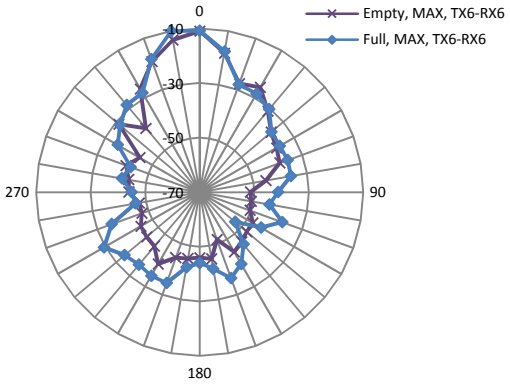

Figure 13 Empty (LOS1) and Full (LOS2) parking lots for TX6-RX6

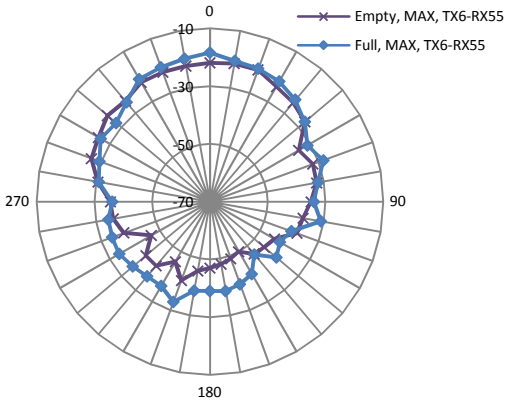

Figure 14 Empty (LOS1) and Full (LOS2) parking lots for TX6-RX55

C. *Outdoor NLOS measurements (Garage)*

Encouraged by the LOS test results, further testing was done in a completely NLOS environment within a parking garage to see if we can maintain communication with purely secondary reflections. The measurement setup for NLOS is similar to the LOS case, except for the use of Θ_t = -25° in elevation and Θ_r= -35, 0, 35°. The selection of these directions were done manually to obtain a good receive signal strength in order to minimize the manual characterization time and effort. For this setup, we also varied the beam widths at the transmitter in addition to the receiver.

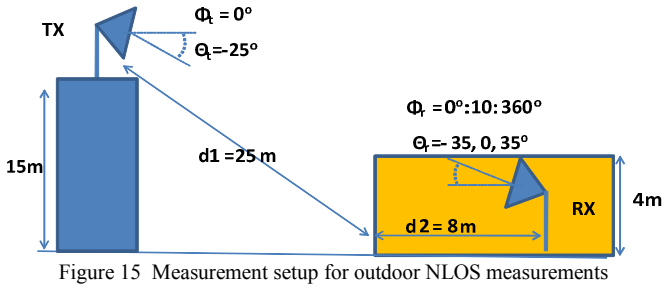

Figure 15 Measurement setup for outdoor NLOS measurements

Figure 16 shows the AoA measurements for received power for 6° HPBW antenna at TX and RX for NLOS. It can be seen that the best performance was obtained at Θ_r = -35° when Φ_r= 0° and Θ_r= 35° when Φ_r = 180°. This implies that good signal strengths were received when the receiver was downtilted to catch the ground reflection at Φ_r = 0° and when the receiver was uptilted to catch the reflections from the ceiling in the opposite direction at Φ_r = 180°.

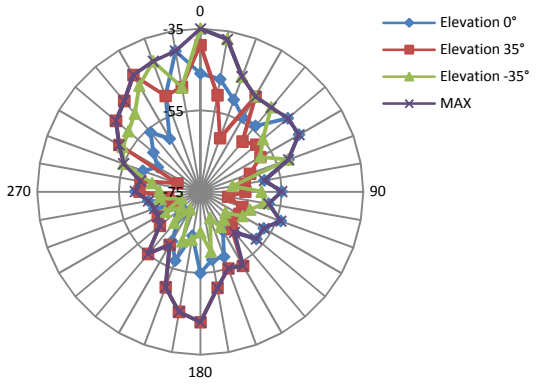

Figure 16 Antenna configuration: TX6-RX6-NLOS

Figure 17 shows the AoA measurements for received power for 6° HPBW antenna at TX and 55° RX for NLOS. It can be seen that the coverage is now more uniform with a wider receive antenna, although there is slight loss in received power along Φ_r = 0° compared to Figure 16.

Figure 18 shows the AoA measurements for received power for 55° HPBW antenna at TX and 6° RX for NLOS. The performance was similar to Figure 16 even though the transmitter now had 12 dB less antenna gain.

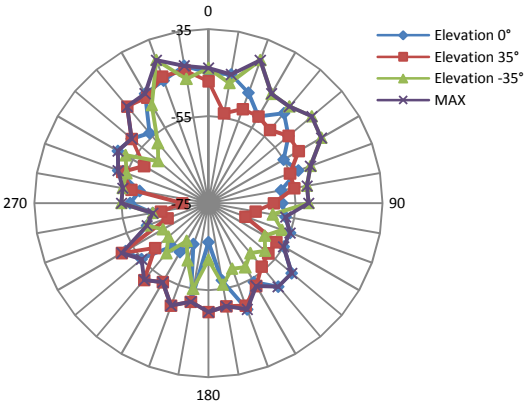

Figure 17 Antenna configuration: TX6-RX55-NLOS

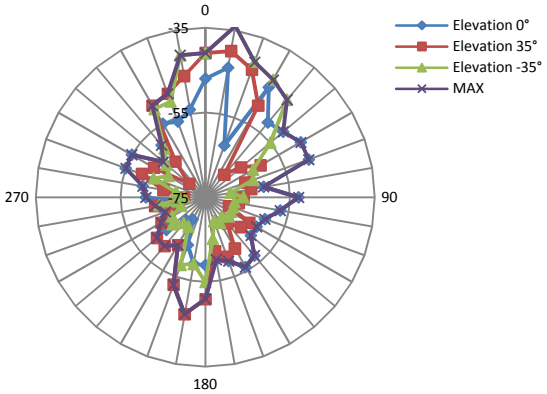

Figure 18 Antenna configuration: TX55-RX6-NLOS

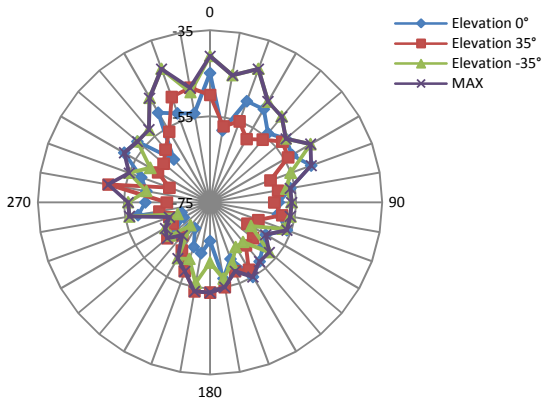

Figure 19 Antenna configuration: TX55-RX55-NLOS

Figure 19 shows the AoA measurements for received power for 55° HPBW antenna at TX and 55° RX for NLOS. The performance was similar to Figure 17 with 12 dB less antenna gain at the transmitter.

Figure 20 provides the comparisons between all the 4 antenna configurations. The shape of the AoA plots seems to be more sensitive to the beam width of the Rx antenna rather than the TX antenna. TX6-RX6 and TX6-RX55 are similar to TX55-RX6 and TX55-RX55 respectively. However, TX6 directs more power toward the RX than TX55. The area enclosed by the TX6-RX6 curve is larger than that enclosed by the TX55-RX6 curve. RX6 provides 5 to 10 dB more gain, than RX55 along the main paths (1st order reflection from the ground around $\Phi_r = 0^o$, and 2nd order reflection from ground than ceiling around $\Phi_r = 180^o$). However, RX55 is better than RX6 along other directions. We expect that mainly scattered waves arrive at the receiver through these directions.

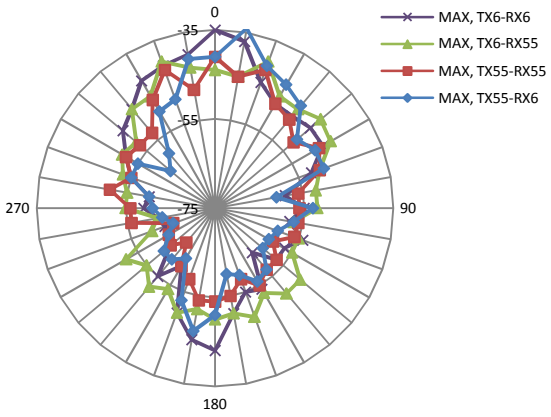

Figure 20 Comparing all 4 NLOS antenna configurations

V. Conclusions And Future Work

A series of experiments is performed to understand the channel feasibility for mmWave NLOS outdoor mobile communication. We first show that water and metal objects are hard to penetrate at these frequencies – however, the energy is not completely absorbed and these objects show substantial reflectivity that could be captured at the mobile receiver. We then perform LOS and NLOS measurements for AoA. We find sufficient scattering even for LOS1 (empty parking lot), and show that a wide HPBW antenna can provide more received power and capture more energy even with a smaller antenna gain, contradictory to conventional use of high gain, small beam width, in mmWave system designs for fixed LOS communication. An equalizer may be needed at the receiver to make use of the additional received power.

These results are preliminary since they have been done only with a few sample points and have been done manually. For true characterization, more data needs to be collected and processed over the entire elevation and azimuth plane at both the TX and RX over a wide range of distances. Currently, we are developing an automated measurement tool for collection of millions of measurement points to demonstrate further feasibility. We also plan to capture other essential information such as delay spread and power delay profiles that have not been discussed in this paper due to equipment limitations, in order to fully characterize the channel. These results will then be used to develop a channel model for outdoor NLOS mmWave mobile communication.

These results, although preliminary, motivate use of these mmWave frequencies with large spectrum availability to provide Gb/s data rates for the next generation of mmWave mobile broadband communication.

VI. Acknowledgment

The authors thank their colleagues at Samsung Electronics, esp. Guowang Miao, for their valuable feedback and discussions and help with channel measurements.

VII. References

[1] Z. Pi and F. Khan, "An introduction to millimeter-wave mobile broadband systems," *Communications Magazine, IEEE*, vol.49, no.6, pg.101-107, Jun. 2011

[2] A. Ghosh, R. Ratasuk, B. Mondal, N. Mangalvedhe and T. Thomas, "LTE-advanced: next-generation wireless broadband technology [Invited Paper]," *Wireless Communications, IEEE*, vol.17, no.3, pg.10-22, Jun. 2010

[3] S. Yong and C. Chong, "An overview of multigigabit wireless through millimeter wave technology: Potentials and technical challenges," *EURASIP Journal on Wireless Communications and Networking*, vol. 2007, no.1, Jan. 2007

[4] S. Geng, J. Kivinen, X. Zhao and P. Vainikainen, "Millimeter-wave propagation channel characterization for short-range wireless communications," *IEEE Transactions on Vehicular Technology*, vol.58, no.1, pg.3–13, Jan. 2009

[5] P. Soma, L. Ong, S. Sun and M. Chia, "Propagation measurements and modeling of LMDS radio channel in Singapore," *IEEE Transactions on Vehicular Technology,* vol.52, no.3, pg.595- 606, May 2003

[6] E. Violette, R. Espeland and K. Allen, "Millimeter-Wave Propagation Characteristics and Channel Performance for Urban-Suburban Environments," NTIA Report 88-239, Dec. 1988

[7] H. Xu, T. Rappaport, R. Boyle and J. Schaffner, "Measurements and models for 38-GHz point-to-multipoint radiowave propagation," *IEEE Journal on Selected Areas in Communications,* vol.18, no.3, pg.310-321, Mar. 2000

[8] H. Xu, V. Kukshya and T. Rappaport, "Spatial and Temporal Characteristics of 60 GHz Indoor Channels," *IEEE Journal on Selected Areas in Communications*, vol.20, no.3, pg.620-630, Apr. 2002

[9] C. Anderson and T. Rappaport, "In-Building Wideband Partition Loss Measurements at 2.5 and 60 GHz," *IEEE Transactions on Wireless Communications*, vol.3, no.3, pg.922-928, May 2004

[10] J. Gilbert et al., "A 4-Gbps Uncompressed Wireless HD A/V Transceiver Chipset," *IEEE Micro*, vol.28, no.2, pg.56-64, March-April 2008